Smart Structures and Systems, *Vol. 25, No. 2 (2020) 229-240*
DOI: https://doi.org/10.12989/sss.2020.25.2.229

Numerical and experimental research on actuator forces in toggled active vibration control system (Part I: Numerical)

Seyyed Farhad Mirfakhraei [1a], Hamid Reza Ahmadi [*2b] and Ricky Chan [3c]

[1] *Department of Civil Engineering, Faculty of Engineering, Seraj University, Tabriz, Iran*
[2] *Department of Civil Engineering, Faculty of Engineering, University of Maragheh, Maragheh, P.O. Box 55136-553, Iran*
[3] *Department of Civil and Infrastructural Engineering, Faculty of Civil Engineering, RMIT University, Melbourne, Australia*

(*Received Feburary 15, 2019, Revised November 11, 2019, Accepted November 29, 2019*)

Abstract. In this research, toggled actuator forces were examined. For achieving to this object, an actuator was installed in a toggle pattern in a S.D.O.F frame and actuator forces were investigated thru a numerical analysis process. Within past twenty years, researchers tried to use strong bracing systems as well as huge dampers to stabilize tall buildings during intensive earthquakes. Eventually, utilizing of active control systems containing actuators to counter massive excitations in structures was emerged. However, the more powerful earthquake excitations, the more robust actuators were required to be installed in the system. Subsequently, the latter process made disadvantage to the active control system due to very high price of the robust actuators as well as their large demands for electricity. Therefore, through a numerical process (Part I), influence of toggled actuator pattern was investigated. The algorithm used in the system was LQR and ATmega328 was selected as a control platform. For comparison, active tendon control system was chosen. The final results show clearly that using the toggle pattern mitigates the required actuator forces enormously leading to deploy much lighter actuators.

Keywords: toggled actuator; control forces; structural active vibration control

1. Introduction

Employing of active control systems has been generated in the past two decades on structures to resist them against seismic (Soong 1988, Yang and Soong 1988, Housner *et al*. 1997, Xu and Teng 2002, Spencer and Nagarajaiah 2003, Xu *et al*. 2014, Dinh *et al*. 2016, Muthalif *et al*. 2017, Zhan *et al*. 2017, Braz-Cesar and Barros 2018). Utilizing high strength material and reliable and precise structure analysing software enables engineers to build more tall and flexible buildings (Yang and Soong 1988, Bayat and Abdollahzadeh 2011, Hejazi *et al*. 2016, Jamnani *et al*. 2017, Bayat *et al*. 2017a, Fu 2018). During the design process, the more strength against the trembling, the more strength and ductility is required for structure (Bayat *et al*. 2010, Bayat and Pakar 2013, Pakar *et al*. 2018). Clearly, the mentioned process is very costly. The bigger cross sections in the structure, the more seismic force attracts onto the members, leading to even bigger sections (Jamnani *et al*. 2018). One of the main advantages of using smart structures is to solve this problem. The efficiency of smart structures has been mentioned in the previous researches and practical installations to protect the structures against the seismic excitations (Ahmadi *et al*. 2015, Bayat *et al*. 2017b). Moreover, in the structures once multiple modes are determinant in its respond, it needs more powerful and adaptive system to resist the structure from intensive excitations and damages (Cheng *et al*. 2008). Also, the many real implementation of active control systems in the world have been reported (Yamazaki *et al*. 1992, Abe and Fujino1994, Spencer and Sain 1997, Wu *et al*. 1997, Cao *et al*. 1998, Kareem *et al*. 1999, Ikeda *et al*. 2001, Yamamoto *et al*. 2001, Ricciardelli *et al*. 2003, Park *et al*. 2006, Tian *et al*. 2017, Gharebaghi and Zangooei 2017, Bagha and Modak 2017, Majeed *et al*. 2018). Furthermore, using of this system in the large civil engineering structures is being extended (Cheng *et al*. 2008). Growing the number of tall buildings in whole of the world makes it inevitable not using active control systems to achieve high reliability and safety (Yang and Soong 1988).

Undoubtedly, achieving optimum control force against the structural response is one of the most important tasks in active control systems. The power and unit cost of actuators as well as their maintenance expenses are very challengeable issues (Liu *et al*. 2003, Amini and Tavassoli 2005, Park *et al*. 2008). The recent researchers have emphasized on mitigation of control forces in active control systems as an efficiency factor in lowering of structural response (Cheng 1988, Pantelides and Cheng 1990, Fisco and Adeli 2011, Miah *et al*. 2015). Furthermore, the importance of actuator positions in active control systems has been reported showing the reduction of the structural response (Pantelides and Cheng 1990, Xu and Teng 2002, Liu *et al*. 2003, Amini and Tavassoli 2005, Rao and Sivasubramanian 2008, He *et al*. 2015).

*Corresponding author, Assistant Professor,
E-mail: ahmadi@maragheh.ac.ir
[a] Ph.D., E-mail: mirfakhraei@seraj.ac.ir
[b] Ph.D., E-mail: ahmadi@maragheh.ac.ir
[c] Ph.D., E-mail: ricky.chan@rmit.edu.au

http://www.techno-press.org/?journal=sss&subpage=7

ISSN: 1738-1584 (Print), 1738-1991 (Online)

The toggle configuration has been known as an competent pattern for viscous damper implementation in a structural system. Utilizing the concept of energy dissipation has been found out via elements installed in the conventional earthquake-resistant structures to protect the structures against excitations (Soong and Dargush 1997, Council 2000, De Domenico and Ricciardi 2018). It has been cited that fluid viscous dampers can strongly increase the damping ratio and decrease the structural vibrations (Constantinou and Symans 1992, Hwang *et al*. 2004, Reinhorn *et al*. 2005, Bayramoglu *et al*. 2014, Ras and Boumechra 2016, Lu *et al*. 2018). Moreover, the practical implementation of these types of dampers can be observed from the work of (Soong and Spencer 2002). However, in a stiff structural system the structural responses are small compared to the flexible one. Therefore, the implementation of viscous damping devices in more stiff structures will be less efficient compare to the flexible structures.

Having the latter difficulty, researchers have recently proposed some configurations for positioning of the dampers to enhance the displacements and velocities in dampers. Taylor in U.S. Patent Nos. 5870863 and 5934028, 1996 (Taylor 1999a, b) has suggested the “toggle-brace-damper” system. An investigation into the “toggle-brace-damper” system has been carried out by (Constantinou *et al*. 2001). This research has confirmed the capability of the system to magnify the axial displacements of damper and the efficiency of energy dissipation via a cyclic loading and shaking table tests in a SDOF steel model. Demanding to have much more free architectural spaces in buildings, another system similar to toggle-brace-damper system, called the “scissor-jack-damper” system, has been presented (Sigaher and Constantinou 2003). Similarly, magnification in displacements and velocity can occur in damper and increase the efficiency of energy dissipation in the frames leading to have more free architectural spaces. One can find some practical examples of this system in (Constantinou *et al*. 2001). One such practical example, that is, 111 Huntington Avenue in Boston, Mass., has a lower toggle system directly pinned to the beam-column joints, which is different from the configuration suggested by Constantinou (Constantinou *et al*. 2001). Besides, Hwang *et al*. (2005) have researched the effect of the lower and upper toggle system in the latter system and the facilitation of the practical installation of the dampers.

In this paper, the upper toggle system that is directly connected to the beam-column joints has been introduced for implementation in an active control system. Unlike the above-mentioned toggle configurations which have been deployed in the passive systems, this research carries out investigations to discover the effect of the toggle pattern in reduction of the active control forces.

Referring to the importance of slight control forces to achieve small-sized actuators for preventing strong earthquake excitations in a structural active control system, an actuator is implemented in the toggle pattern in an active control system in the single-degree-of-freedom (SDOF) shear frame. This research Experimental and numerical investigation are carried out using the latter system to explore effect of this configuration on the actuator forces regarding to the different earthquake excitations.

Fig. 1 shows a single-degree-of-freedom shear frame having one span and one storey. As it is clear, the actuator has been implemented in a toggle configuration, i.e., eb member. Members ea and ec are assumed to be rigid axially. The members ea and ec are connected to the main frame and each other at hinged points a, c and e, respectively. It means that the movement of members ea, ec and eb has been located in the plane of the frame abcd. Also, there is a response sensor at the top of the frame. Furthermore, a controller has been installed in this system that can determine the control signals by its own algorithm based on the received structural response data gained by the sensor.

In this system, the structural response i.e., velocities and displacements due to earthquake excitations is measured by the sensor. Then, the gained signals are sent to the controller. Furthermore, based on the controller algorithm, the control forces are calculated and the signals sent to the actuator. Finally, the control forces are applied by the actuator to the main structure through the members ea and ec to counteract the effect of that disturbance in the frame.

The internal forces in the toggle pattern in the active control system have been shown in Fig. 2. In this sketch x(t) is actuator force, $F_1(t)$ and $F_2(t)$ are tension or compression forces in members ea and ec respect to the direction of the displacement, M is a lumped mass of the structure and $\ddot{S}_g(t)$ is the earthquake acceleration.

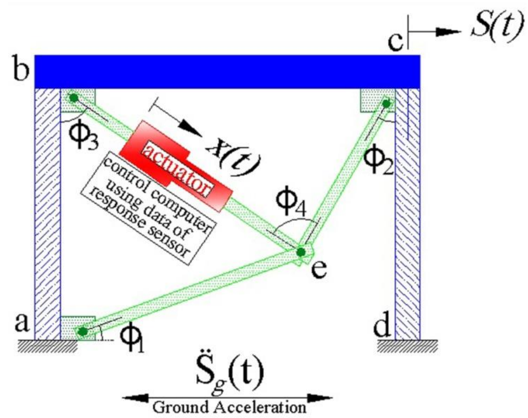

Fig. 1 Configuration of toggle in active control system

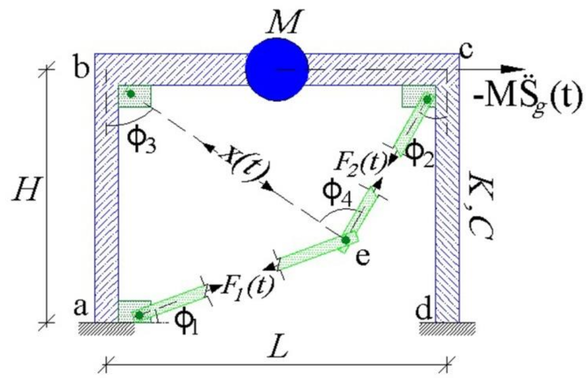

Fig. 2 Existing forces of toggle in active control system

2. Motion equation

Using Fig. 2, the equilibrium of forces in the hinge e in a horizontal direction in a time instant can be derived as follows

$$F_2(t)Sin\varphi_2 - F_1(t)Cos\varphi_1 + x(t)Sin\varphi_3 = 0 \tag{1}$$

where, x(t) is actuator force, F_1(t) and F_2(t) are tension forces in the members of ea and ec, respectively. Also, the angles of ϕ_1, ϕ_2 and ϕ_3 have been shown in Fig. 2. Similarly, the equilibrium of forces in the hinge e in a vertical direction is derived as below

$$F_2(t)Cos\varphi_2 - F_1(t)Sin\varphi_1 + x(t)Cos\varphi_3 = 0 \tag{2}$$

By solving Eqs. (1) and (2) simultaneously, F_1(t) and F_2(t) can be resulted as below

$$F_1(t) = \alpha_1 x(t), \qquad F_2(t) = \alpha_2 x(t) \tag{3}$$

where, Ω_1 and Ω_2 are as follows

$$\Omega_1 = \frac{Sin(\varphi_2 + \varphi_3)}{Cos(\varphi_1 + \varphi_2)}, \quad \Omega_2 = \frac{Cos(\varphi_1 - \varphi_3)}{Cos(\varphi_1 + \varphi_2)} \tag{4}$$

Assuming M, C, and K are the lumped mass, damping and stiffness of the structure, respectively. the motion equation of the aforementioned system applying the dynamic equilibrium is gained as follows

$$M\ddot{S}(t) + C\dot{S}(t) + KS(t) + x(t)Sin\varphi_3 + F_2Sin\varphi_2 = -m\ddot{S}_g(t) \tag{5}$$

Using Eqs. (3), (4) and (5), the motion equation for the toggle system is gained as

$$M\ddot{S}(t) + C\dot{S}(t) + KS(t) = -\Omega x(t) - M\ddot{S}_g(t) \tag{6}$$

in which

$$\Omega = Sin\varphi_3 + \frac{Cos(\varphi_1 - \varphi_3)}{Cos(\varphi_1 + \varphi_2)}Sin\varphi_2 \tag{7}$$

Eq. (6) shows the motion equation for an active control system in the toggle configuration, illustrated in Fig. 2. In this formula, M, C, K, x(t) and $\ddot{S}_g(t)$ are the mass, the damping coefficient, the stiffness, the actuator force and the earthquake acceleration, respectively. In addition, their dimension are equal to ${kNs^2}/{m}$,${kNs}/{m}$, ${kN}/{m}$, kN and ${m}/{s^2}$, respectively. Besides, Ω is the toggle coefficient, which depends on the angles of ϕ_1, ϕ_2 and ϕ_3. Eq. (6) dictates the motion of the system for toggle configuration. From the control system design point of view, the objective is to minimize the displacement S(t) by changing the force x(t). The variable $\ddot{S}(t)$ is the acceleration produced by an earthquake excitation, which is determined to be disturbance.

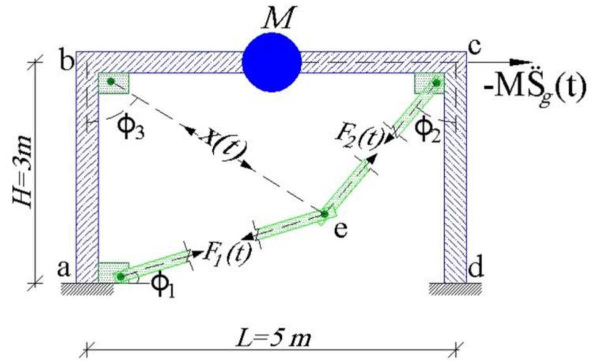

Fig. 3 Control system of active toggle

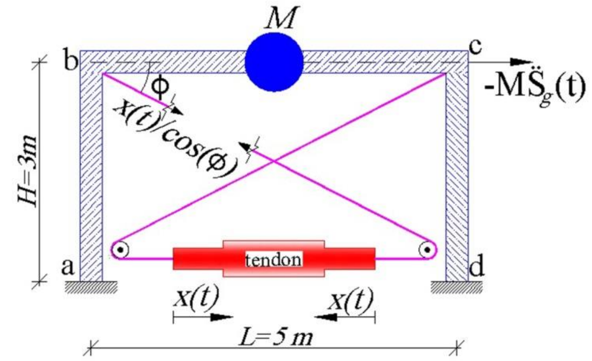

Fig. 4 Control system of active tendon

3. Efficiency of toggle in active control system

One of the main objectives of this research is mitigation of the required active control forces inserted by the actuators. This mitigation of control forces is considered as an efficiency factor in the active toggle control system. Therefore, to investigate this efficiency, two systems with a single-degree-of-freedom having identical mass, damping and stiffness values are chosen. The first system is the active control system in a toggle pattern and the second one is a tendon control system (Cheng *et al*. 2008), as illustrated in Figs. 3 and 4, respectively.

The motion equation of the active toggle control system is restated here, as below

$$M\ddot{S}(t) + C\dot{S}(t) + KS(t) = -\Omega x_{Toggle}(t) - M\ddot{S}_g(t) \tag{8}$$

Also, the motion equation of the active tendon control system, shown in Fig. 4, is as follows (Cheng *et al*. 2008).

$$M\ddot{S}(t) + C\dot{S}(t) + KS(t) = -x_{Tendon}(t) - M\ddot{S}_g(t) \tag{9}$$

Utilizing Eqs. (8) and (9), the relationship between the actuator forces in these two systems, i.e., toggle and tendon systems is derived as below

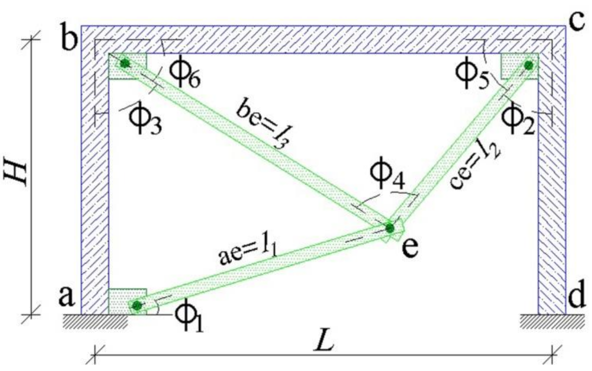

Fig. 5 The parameters of toggle configuration in active control system

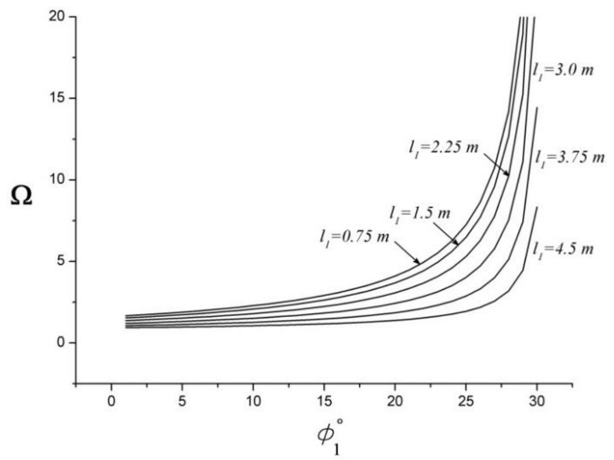

Fig. 6 Variations of Ω to ϕ_1 with different l_1

$$x_{Toggle}(t) = \left(\frac{1}{\Omega}\right) x_{Tendon}(t) \tag{10}$$

where Ω is the toggle coefficient, described in Eq. (7).

In Eq. (10), the coefficient Ω plays important role to show the efficiency of the active toggle control system. Here, if Ω is greater than unity, then the toggle system becomes more efficient than the tendon system. Thus, to prove this, one should find the variation of Ω for all the acceptable values of ϕ_1.

In the following, it is proved that all values of Ω are greater than unity. Therefore, the control forces in the toggle control system are Ω times smaller than the control forces in the tendon control system for balancing the frame against the same excitation.

One can see from Figs. 5 and 6 that approaching ϕ_1 to its maximum values causes to increase the toggle coefficient Ω rapidly. However, during the design process, the condition for establishing of toggle configuration, i.e., $\phi_1 + \phi_2 < 90°$, as well as manufacturing restrictions, should be noticed.

4. Investigation of the effect of Ω

Using the geometry of the system in the toggle pattern shown in Fig. 2, for any given value for ϕ_1, the corresponding value for ϕ_2 can be calculated. However, the appropriate establishing of the motion equation in the toggle system relies on proper values for ϕ_1 to ϕ_3 and l_1. Otherwise, operating of the active control system having the toggle configuration cannot be valid anymore. It must be cited that the system performs as a toggle configuration in the active control system if $\phi_1 + \phi_2 < 90°$.

On the other hand, ϕ_1 and l_1 are independent values in the toggle configuration. It means that after setting values for ϕ_1 and l_1, one can calculate the all other geometrical characteristics using the system geometry. Noticing Fig. 5, the latter values can be attained by the following formulas

$$\begin{aligned} l_2 &= \sqrt{(L^2 + l_3^2 - 2Ll_3Cos(\varphi_6)} \\ l_3 &= \sqrt{(H^2 + l_1^2 - 2Hl_1Cos(90 - \varphi_1)} \end{aligned} \tag{11}$$

$$\begin{aligned} \varphi_3 &= arcCos\left(\frac{-l_1^2 + H^2 + l_3^2}{2Hl_3}\right) \\ \varphi_5 &= arcCos\left(\frac{-l_3^2 + L^2 + l_2^2}{2Ll_2}\right) \end{aligned} \tag{12}$$

$$\varphi_2 = 90 - \varphi_5, \qquad \varphi_6 = 90 - \varphi_3 \tag{13}$$

The effect of variations of ϕ_1 and l_1 is due to the coefficient of Ω which is direct multiplication factor to the actuator force, as indicated in Eq. (6). Hence, numerically gaining variations of Ω with respect to ϕ_1 using Eq. (7), can be more straightforward. Therefore, having H = 3 m and L = 5 m in Fig. 3, the variations of Ω with respect to ϕ_1 having different l_1 can be calculated. Note that the maximum values of ϕ_1 and ϕ_2 can be easily attained using Fig. 3. However, as a toggle establishment criterion stated earlier, the inequality of $\phi_1 + \phi_2 < 90°$ should be satisfied. So, the maximum values for ϕ_1 and ϕ_2 are calculated 30.96° and 59.04°, respectively.

Utilizing Eq. (7), while l_1 changes from 0.5 m to 4.0 m, all values of Ω have been gained respect to all satisfying values of ϕ_1. These results are plotted in Fig. 6.

The all values of Ω are greater than unity, as it is obvious from Fig. 6. Therefore, regarding to the efficiency of the toggle system compared to the tendon system, these greater than unity values of Ω confirm that the toggle system is more efficient than the tendon system.

5. Investigating the effect of variables in toggle configuration

It was mentioned in previous section that ϕ_1 and l_1 are self-standing values in the toggle pattern. The meaning is that the two aforementioned parameters must be selected before designing of the active control system in a toggle pattern. This is the reason that makes it very important to choose the proper values for these two parameters.

Fig. 6 shows that, when the value of ϕ_1 reaching to its maximum value, the toggle coefficient of Ω raises sharply. So, in ϕ_1s that are getting close to their maximum values, the toggle system operates more efficiently. Although

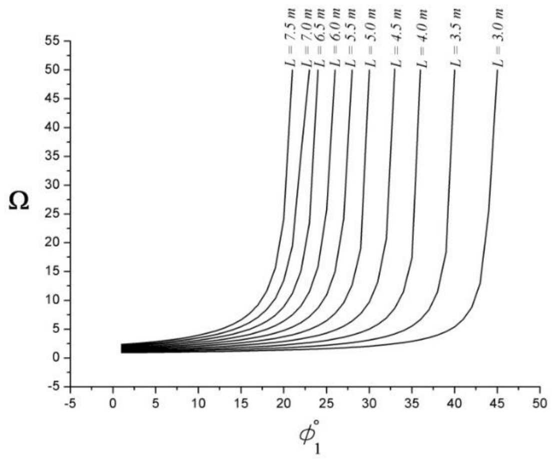

Fig. 7 Variations of Ω to ϕ_1 with different L

attaining the higher toggle coefficient is beneficial, one should take into consideration the toggle establishment criterion $\phi_1 + \phi_2 < 90°$ and construction limitations as well as selecting ϕ_1.

Moreover, the results plotted in Fig. 6 can guide designers to select the optimum value for l_1 considering their construction specifications and conditions. It is obvious from Fig. 6 that the smaller l_1 produces the greater Ω. Accordingly, selecting the smaller l_1 enhances the efficiency of the toggle system.

To research the effects of changes of the frame height, H, on the toggle coefficient, the similar numerical procedure utilized in prior section is applied here. So, selecting L = 6.0 m and l_1 = 1.5 m in Fig. 3, the changes of Ω with respect to ϕ_1 having different H can be determined. One can find the outcomes in Fig. 8.

Similar to the previous section, to consider the effects of changes of the frame span length, L, on the toggle coefficient, the numerical procedure is performed here as well. For this purpose, choosing H = 3.0 m and l_1 = 1.5 m in Fig. 3, the changes of Ω with respect to ϕ_1 having different l can be calculated. The Fig. 7 shows the result. Fig. 7 indicates that the bigger span generates the greater toggle coefficient of Ω while ϕ_1 changes from zero degree to its relevant maximum value. From this graph, one can see that it is desirable to deploy the frames with bigger spans through the design process in the active toggle control system.

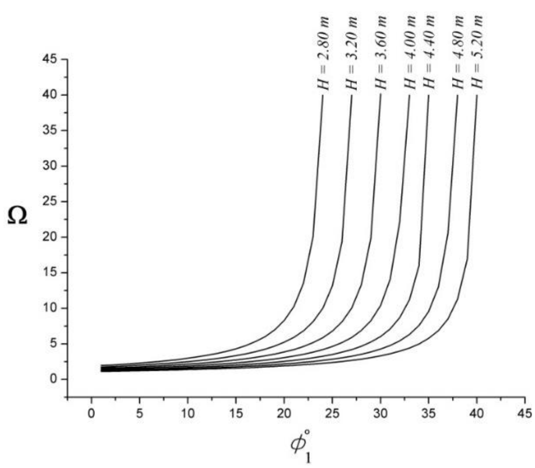

Fig. 8 Variations of Ω to ϕ_1 with different H

Fig. 8 illustrates that the bigger height generates the smaller toggle coefficient of Ω while ϕ_1 changes from zero degree to its relevant maximum value. From this graph, one can see that in the range of acceptable ϕ_1s, it is desirable to deploy the frames with smaller storey height as much as possible through the design process in the active toggle control system.

6. Numerical procedure

Considering the main objectives indicated in this investigation, the mitigation of the required control forces in the active toggle control system is researched here using a numerical analysis. The summary of this process is as follows:

(a) Selecting a SDOF active toggle control system, shown in Fig. 3 as a main system.
(b) Choosing a SDOF active tendon control system, indicated in Fig. 4 as a comparison system.
(c) Calculating the optimum value for toggle coefficient Ω considering the toggle pattern property.
(d) Expressing the applied feedback control layout in the both systems. Explaining the installed algorithm in both systems.
(e) Selecting the earthquake acceleration data and gaining the state form of the motion equation for both systems.
(f) Getting the gain matrix using the LQR function in MATLAB® and determining the state vector utilizing LSIM function in MATLAB®.
(g) Determining the control forces for both systems.
(h) Checking the outcomes utilizing the produced graphs.

6.1 Control system of active toggle and active tendon

In this process, a SDOF frame with an active toggle control system is chosen, as illustrated in Fig. 3. The whole system including structure, actuator, sensor and controller in this procedure are presumed to be linear (Chung *et al*. 1988, 1989, 2008, Cheng and Jiang 1998a, b).

Through this numerical analysis process, the columns are selected 150UC23.4 and the beam is chosen 180UB22.2. The regarding characteristics are set in the Table 1.

Presuming the damping ratio of 2% for a steel frame, i.e., ζ = 2%, the stiffness, damping, natural frequency and period of the considered frame has been worked out utilizing the below formulas, respectively (Chopra 2017)

$$K = \frac{24EI}{H^3}\frac{12\rho + 1}{12\rho + 4} \tag{14}$$

Table 1 Characteristics of toggle system

Specification	Value	Unit
M	12	*ton*
C	3.4	*kNs/m*
K	589	*kN/m*
I_b	15.3×10^6	mm^4
I_c	3.98×10^6	mm^4
ρ	1.153	—
E	200	*GPa*
T_n	0.898	*sec*

$$\rho = \frac{EI_b/L}{2EI_c/H} \tag{15}$$

In the aforementioned formulas, L, H, K, I_b, I_c , ρ and E are the frame span, height, stiffness, the moment of inertia of the beam, the moment of inertia of the columns, the beam-to-column stiffness ratio and modulus of elasticity of steel, respectively.

To have a checking system, an active tendon control system with the same characteristics as those shown in Table 1 is taken. This system has been indicated in Fig. 4 (Cheng *et al*. 2008). All the specifications of this system apart from the type of control system, are presumed to be similar to the toggle system.

As explained in the previous section, the characteristics of tendon system have been considered similar to the active toggle control system, as indicated in Fig. 4. It was already indicated that the greater values of toggle coefficient Ω create the smaller actuator forces. Also, one can see from Fig. 6 that the toggle coefficient of Ω raises by decreasing the length of the lower brace l_1. Accordingly, the smaller values of l_1 generate the bigger values of Ω, which leads to gain slighter control forces. For attaining the optimum values of Ω, both the formation criterion for the toggle pattern and the construction restrictions must be considered. Therefore, noticing to Fig. 6, ϕ_1 and l_1 are set as 27° and 1.5 m, respectively. Regarding to prior explanation, ϕ_1 and l_1 are self-standing values. So, after selecting the optimum values for ϕ_1 and l_1, the remain specifications of the system can be calculated. All the required characteristics for obtaining the optimum toggle coefficient in this process have been worked out using the equations noted in Section 4 and indicated in Table 2. Finally, the toggle coefficient of Ω is gained utilizing by Eq. (7).

State form of motion equation of the control system is indicated as below (Cheng *et al*. 2008)

$$\left[\dot{Y}(t)\right] = [\alpha][Y(t)] + [\beta_u][x(t)] + [\beta_r]\left[\ddot{S}_g(t)\right] \tag{16}$$

in which

$$\left[\dot{Y}(t)\right] = \begin{bmatrix}\dot{S}(t)\\ \ddot{S}(t)\end{bmatrix}_{2n\times1} \tag{17}$$

$$\alpha = \begin{bmatrix}[0] & [I]\\ -[M]^{-1}[K] & -[M]^{-1}[C]\end{bmatrix}_{2n\times2n} \tag{18}$$

Table 2 Features to calculate optimum Ω

Specification	Value	Unit
l_1	1.5	*m*
l_2	4.33	*m*
l_3	2.68	*m*
ϕ_1	27	*degree*
ϕ_2	57.7	*degree*
ϕ_3	30	*degree*
ϕ_4	87.7	*degree*
ϕ_5	32.3	*degree*
ϕ_6	60	*degree*
Ω	9.6	—

$$[\beta_u] = \begin{bmatrix}[0]\\ [M]^{-1}[\gamma]\end{bmatrix}_{2n\times r} \tag{19}$$

$$[\beta_r] = \begin{bmatrix}[0]\\ [M]^{-1}[\delta]\end{bmatrix}_{2n\times 1} \tag{20}$$

Utilizing the closed-loop feedback control layout, Eq. (16) can be mathematically worked out. Next, the control force vector is resulted by feeding back the structural response measurements. Note that in the aforementioned equations, n is the number of storeys and r is the number of actuators. Therefore, the feedback law can be expressed as follows.

$$[x(t)]_{r\times1} = -[\Psi]_{r\times2n}[Y(t)]_{2n\times1} \tag{21}$$

In Eq. (21), [Ψ] is feedback gain matrix with a dimension of r×2n. Using these r extra equations, the control system response, i.e., [Y(t)], can be gained from Eq. (16). Substituting Eq. (21) into Eq. (16), results to the following equation

$$\left[\dot{Y}(t)\right] = [\alpha_c][Y(t)] + [\beta_r]\left[\ddot{S}_g(t)\right] \tag{22}$$

in which

$$[\alpha_c] = [\alpha] - [\beta_u][\Psi] \tag{23}$$

In Eq. (23), matrix $[\alpha_c]$ is known as the closed-loop plant matrix of the system. As mentioned above, if all the state variables of the system are determined, the closed-loop system would be converted to a full-state feedback (Cheng *et al*. 2008).

In smart structures, determining the state variables, i.e., displacements and velocities, is not straightforward. In a proper using of instruments, determining the accelerations is a very confident method in seismic response control systems. However, some research showed that the gaining of direct acceleration feedback was possible (Spencer *et al*. 1993, Dyke *et al*. 1994a, b, 1996a, b). Utilizing this procedure makes convenient in the sensing system, which results the attainment of more practical control systems.

It should emphasise that the closed-loop feedback control layout is the most well-known and convenient feedback control layout in smart structures. In this

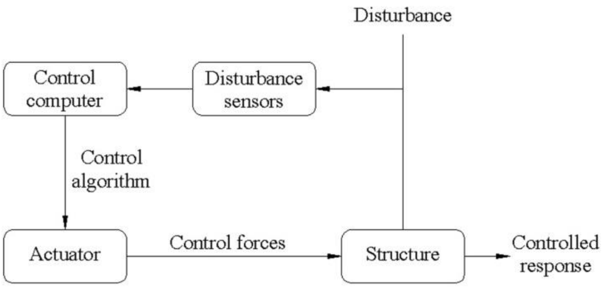

Fig. 9 Designed flowchart for closed-loop control

numerical procedure, the closed-loop feedback control layout has been chosen to be deployed in both systems, i.e., the toggle and tendon control systems (Cheng *et al*. 2008). One can see the schematic sketch of closed-loop control in Fig. 9.

The active control force is gained utilizing active control algorithms via the measured structural response. The control algorithms are set in electronic devices known as either digital controller or control computer. Also, control law is the mathematical model of the controller for the active control systems. Moreover, insertion of the control algorithm in an active control system is called controller design. In this research, well-known algorithms of LQR and pole placement have been utilized through the especial functions in MATLAB® (Cheng *et al*. 2008).

6.2 Using control matrix in active toggle and tendon control system

The earthquake acceleration records which has been deployed in both active control systems are 1979 Imperial Valley–El Centro M (6.5) and 1994 Northridge M (6.7). The first 20 seconds of these earthquake accelerations are indicated in Fig. 10. These data are available in the website of the Pacific Earthquake Engineering Research Centre.

The state form of motion equation for the active toggle control system is achieved as follows. Note that in these equations, $\Omega = 9.6$ is the toggle coefficient that has been previously worked out.

$$\left[\dot{Y}(t)\right] = [\alpha]_c[Y(t)] + [\beta_r]\left[\ddot{S}_g(t)\right], \quad [\beta_r] = \begin{bmatrix} [0] \\ [M]^{-1}[\delta] \end{bmatrix}_{2n\times 1} \tag{24}$$

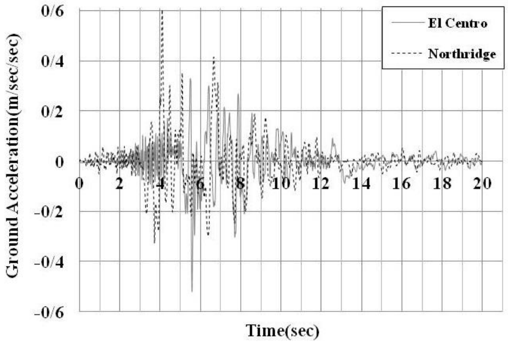

Fig. 10 Time-history of El Centro and Northridge earthquakes

$$[\alpha_c] = [\alpha] - [\Omega\beta_u][\Psi] \tag{25}$$

$$[\alpha] = \begin{bmatrix} 0 & 1 \\ \frac{-598}{12} & \frac{-3.4}{12} \end{bmatrix} \tag{26}$$

$$[\beta_u] = \begin{bmatrix} 0 \\ -\Omega\frac{1}{12} \end{bmatrix} \tag{27}$$

For achieving the control gain matrix [Ψ] in the closed-loop control system, the function of LQR in MATLAB® software is utilized as below

$$[\Psi] = LQR(\alpha, \beta_u, \kappa, \lambda) \tag{28}$$

In Eq. (28), matrices [κ] and [λ] are called weighting matrices and in this calculation procedure are set to be as follows. Also, the other terms have been already explained.

$$[\kappa] = \begin{bmatrix} 10 & 0 \\ 0 & 10 \end{bmatrix}, \qquad [\lambda] = [0.001] \tag{29}$$

Utilizing the PLACE function in MATLAB®, for attaining the more stability of the system, poles of the system are designed to be –150, identically. Therefore, the gain matrix for the closed-loop control system is as follows

$$\left[\Psi_{Toggle}\right] = [-28114 \quad -375] \tag{30}$$

Calculating the gain matrix in the active tendon control system would be similar to the process explained for the active toggle control system. Therefore, utilizing the same poles, the gain matrix in active tendon control system is obtained as follows

$$[\Psi_{Tendon}] = \Omega\left[\Psi_{Toggle}\right] = 9.6\left[\Psi_{Toggle}\right] \tag{31}$$

6.3 Calculation of structural displacement response and control forces

One can easily achieve the state vector [Ψ(t)] which comprises the displacements and velocities utilizing LSIM function in MATLAB® software package. In an optimal closed-loop control system, optimal control force [x(t)] is regulated based only on the feedback of [Ψ(t)]. So, to achieve the state vector, the related response in the structure should be measured at time instant t by implementing the displacement and velocity sensors at the proper locations on the floor.

As the characteristics of the two systems, i.e., toggle and tendon systems, have been assumed the same, the attained structural displacement responses for both systems would be identical. These structural responses related to the deployed earthquake accelerations can be worked out utilizing the function LSIM in MATLAB® software as follows

$$[Z, Y] = LSIM(\alpha_c, \beta_r, W, \ddot{S}_g, Q) \tag{32}$$

In the above equation, α_c is named the closed-loop plant

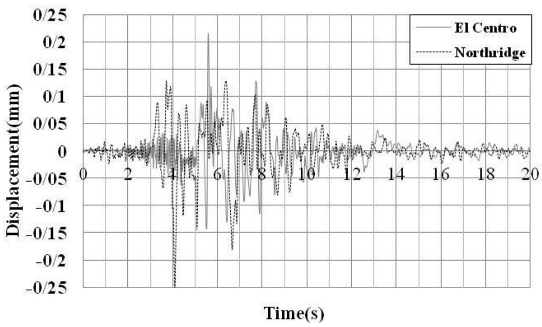

Fig. 11 The displacements of top of the frames for El Centro and Northridge earthquakes

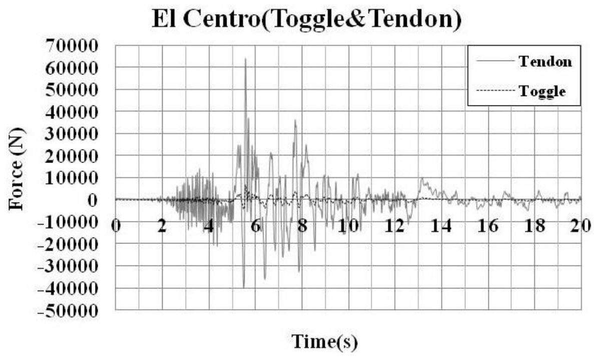

Fig. 12 Comparison between control forces in El Centro Earthquake

matrix of the system, β_r and $\ddot{S}_g(t)$ have been already expressed in the prior sections. Also, matrices $W = [1 \quad 1]$ and Q are the sensor matrix and the simulation time matrix, respectively. The structural displacement responses, i.e., the displacements of top of the frames for 1979 El Centro and 1994 Northridge earthquakes, are indicated in Fig. 11. The absolute maximum controlled structural displacement under 1979 El Centro and 1994 Northridge earthquakes are 0.22 mm and 0.25 mm, respectively.

After attaining the control gain matrix, the demanded control forces for both systems can be calculated utilizing Eq. (21). Note that in this equation, the control gain matrix has been achieved by utilizing LQR algorithm. Therefore, the equation for calculating the control forces in both systems is considered as follows

$$[x(t)] = -[\Psi][Y(t)] \tag{33}$$

In the aforementioned equation, the matrices [Ψ] and [Y(t)] have already been achieved for the relevant systems individually, as explained in the prior sections.

7. Results comparison for numerical procedure

7.1 Forces

Hence, after calculating the control forces or, in the other words, the actuator forces in the active toggle and tendon control systems, these control forces have been shown on graphs in Figs. 12 and 13 to display the difference between the relevant results.

From the figures, it is obviously seen that an active control system with the toggle pattern can enormously decrease the demanded actuator forces. In this numerical research, this mitigation is about 89.6%, compared to the tendon control system with various seismic excitations. However, considering the toggle coefficient, this mitigation amount in the control forces in the toggle system can be attained immediately from Eq. (10).

7.2 Displacements

The results comparison due to the controlled and uncontrolled displacements have been shown in Figs. 14 and 15 for El Centro and Northridge earthquakes,

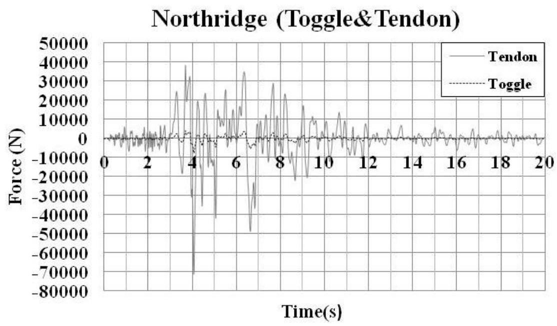

Fig. 13 Comparison between control forces in Northridge Earthquake

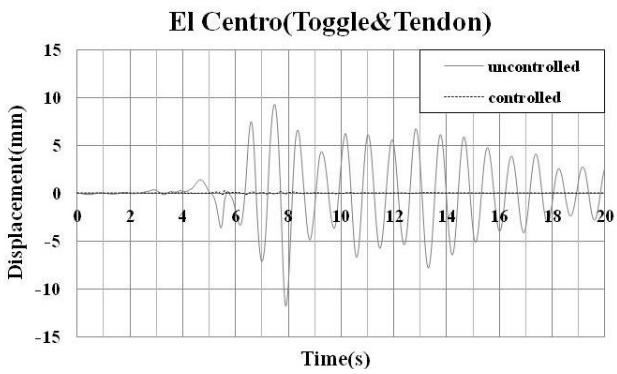

Fig. 14 Comparison between controlled and uncontrolled displacements in El Centro earthquake

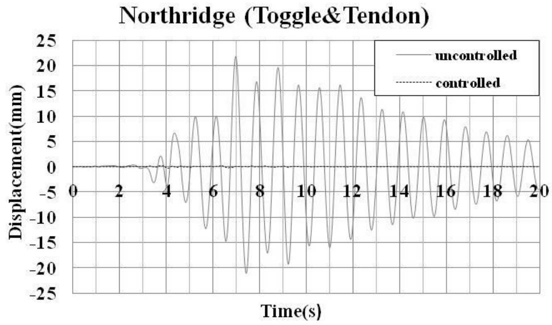

Fig. 15 Comparison between controlled and uncontrolled displacements in Northridge earthquake

respectively. The responses for the free vibration have been determined by the methods based on interpolation of excitation (Mahdavi *et al*. 2012, Bayat and Pakar 2015, Chopra 2017, Ahmadi and Anvari 2018, Ahmadi *et al*. 2019).

It is clear from Figs. 14 and 15 that utilizing the toggle pattern in an active control system can strongly decrease the structural responses under the earthquake excitations.

8. Experimental model

In this research, it was decided to use the small-scale model so that the experiment test could be carried out utilizing a proper small shaking table. In fact, a laboratory model was developed to ensure numerical computation and evaluation of the proposed toggled actuator forces. As is clear from Fig. 16, the active toggle control experimental model was built manually in the laboratory of RMIT University. This model consists of four columns and a rigid ceiling connected to the columns. The material of the columns and ceiling are made of aluminum and timber,respectively. The columns, which are attached to the timber base, were selected to be flexible enough to be vibrated easily during the shaking on the shaking table. The ceiling was chosen rigid enough to transverse the vibration consistently to the four columns and follow the theoretical concept of the single-storey frame vibration. The connections of the columns with the ceiling and floor are considered fixed end. The specifications of the experimental frame are indicated in Table 3.

The full description of the laboratory tests and evaluation of the results will be presented in Part II.

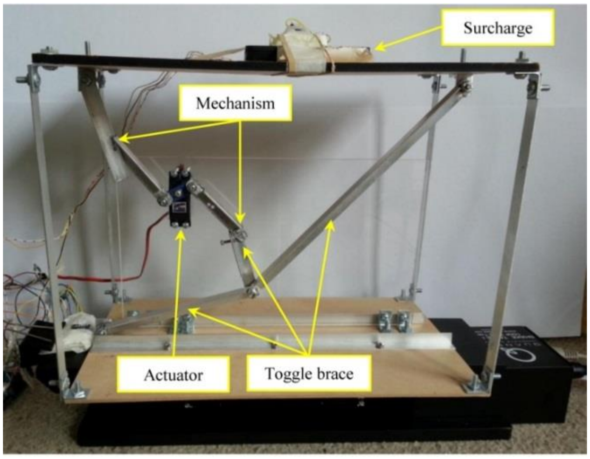

Fig. 16 Experimental model

Table 3 Frame specifications

Explanation	Symbol	Value	Unit
Span length	L	0.346	m
Width	W	0.202	m
Height	H	0.258	m
Lower brace	l_1	0.150	m
Upper brace	l_2	0.294	m
Angle between lower brace and floor	ϕ_1	17.5	degree
Angle between upper brace and right column	ϕ_2	43.6	degree
Angle of control force	ϕ_3	33.9	degree
Mass	M	1.094	kg
Stiffness	K	169.4	N/m
Damping	C	0.184	Ns/m
Toggle coefficient	Ω	1.93	—

9. Conclusions

In this paper, the toggled actuator forces in active vibration control system was examined. The gained results prove that the insertion of the toggle pattern in a S.D.O.F shear frame in an active control system creates coefficient Ω which is direct factor to the control force in the motion equation. The value of coefficient Ω is greater than unity in general engineering frames. Moreover, the results show that the higher toggle coefficient Ω produces the lighter control forces. Also, this investigation uncovers that the parameters of ϕ_1 and l_1 are independent values. These values must be assumed correctly before finding of the other system characteristics. Besides that, the correct creation of the motion equation in the toggle system depends on proper values for ϕ_1 to ϕ_3 and l_1. Moreover, the condition of the system to work in a toggle pattern is $\phi_1 + \phi_2 < 90°$. Also, the research denotes that the lower brace length, i.e., l_1, plays an important role in the toggle pattern. Since the smaller l_1 creates the greater Ω, then its smaller values are more desirable. Furthermore, this investigation reveals that choosing a frame with greater span has an advantageous in the system, since the bigger span generates the greater toggle coefficient Ω. On the other hands, the outcomes emphasize on the frame height to be as short as possible, that is due to producing the smaller toggle coefficient Ω by the greater heights. The outcomes of this research also indicate that one can reach to more capable toggle system using the values of ϕ_1s close to its maximum values. However, consideration should take into account about the construction limitations as well as the toggle creation condition, i.e., $\phi_1 + \phi_2 < 90°$. In addition, comparing results in the toggle and tendon actuator forces prove 89.6% reduction for the former. Consequently, utilizing the toggle system enormously mitigates the actuator forces leading to have much smaller actuator with lower price.

References

Abe, M. and Fujino, Y. (1994), "Dynamic characterization of multiple tuned mass dampers and some design formulas", *Earthq. Eng. Struct. Dyn.*, **23**(8), 813-835. https://doi.org/10.1002/eqe.4290230802

Ahmadi, H.R. and Anvari, D. (2018), "Health monitoring of pedestrian truss bridges using cone-shaped kernel distribution", *Smart Struct. Syst., Int. J.*, **22**(6), 699-709.

https://doi.org/10.12989/sss.2018.22.6.699

Ahmadi, H.R., Daneshjoo, F. and Khaji, N. (2015), "New damage indices and algorithm based on square time–frequency distribution for damage detection in concrete piers of railroad bridges", *Struct. Control Health Monitor.*, **22**(1), 91-106. https://doi.org/10.1002/stc.1662

Ahmadi, H.R., Namdari, N., Cao, M. and Bayat, M. (2019), "Seismic investigation of pushover methods for concrete piers of curved bridges in plan", *Comput. Concrete, Int. J.*, **23**(1), 1-10. https://doi.org/10.12989/cac.2019.23.1.001

Amini, F. and Tavassoli, M.R. (2005), "Optimal structural active control force, number and placement of controllers", *Eng. Struct.*, **27**(9), 1306-1316. https://doi.org/10.1016/j.engstruct.2005.01.006

Bagha, A.K. and Modak, S.V. (2017), "Feedback control strategies for active control of noise inside a 3-D vibro-acoustic cavity", *Smart Struct. Syst., Int. J.*, **20**(3), 273-283. https://doi.org/10.12989/sss.2017.20.3.273

Bayat, M. and Abdollahzadeh, G. (2011), "On the effect of the near field records on the steel braced frames equipped with energy dissipating devices", *Latin Am. J. Solids Struct.*, **8**(4), 429-443. http://dx.doi.org/10.1590/S1679-78252011000400004

Bayat, M. and Pakar, I. (2013), "On the approximate analytical solution to non-linear oscillation systems", *Shock Vib.*, **20**(1), 43-52. https://doi.org/10.3233/SAV-2012-0726

Bayat, M. and Pakar, I. (2015), "Mathematical solution for nonlinear vibration equations using variational approach", *Smart Struct. Syst., Int. J.*, **15**(5), 1311-1327. https://doi.org/10.12989/sss.2015.15.5.1311

Bayat, M., Shahidi, M., Barari, A. and Domairry, G. (2010), "On the approximate analysis of nonlinear behavior of structure under harmonic loading", *Int. J. Phys. Sci.*, **5**(7), 1074-1080.

Bayat, M., Daneshjoo, F., Nistico, N. and Pejovic, J. (2017a), "Seismic evaluation of isolated skewed bridges using fragility function methodology", *Comput. Concrete, Int. J.*, **20**(4), 419-427. https://doi.org/10.12989/cac.2017.20.4.419

Bayat, M., Pakar, I. and Bayat, M. (2017b), "Nonlinear vibration of multi-body systems with linear and nonlinear springs", *Steel Compos. Struct., Int. J.*, **25**(4), 497-503. https://doi.org/10.12989/scs.2017.25.4.497

Bayramoglu, G., Ozgen, A. and Altinok, E. (2014), "Seismic performance evaluation and retrofitting with viscous fluid dampers of an existing bridge in Istanbul", *Struct. Eng. Mech., Int. J.*, **49**(4), 463-477. https://doi.org/10.12989/sem.2014.49.4.463

Braz-Cesar, M.T. and Barros, R. (2018), "Semi-active fuzzy based control system for vibration reduction of a sdof structure under seismic excitation", *Smart Struct. Syst., Int. J.*, **21**(4), 389-395. https://doi.org/10.12989/sss.2018.21.4.389

Cao, H., Reinhorn, A.M. and Soong, T.T. (1998), "Design of an active mass damper for a tall TV tower in Nanjing, China", *Eng. Struct.*, **20**(3), 134-143.

Cheng, F.Y. (1988), "Response control based on structural optimization and its combination with active protection", *Procedings of the World Conference on Earthquake Engineering*, Tokyo-Kyoto, Japan, August.

Cheng, F.Y. and Jiang, H. (1998a), "Hybrid control of seismic structures with optimal placement of control devices", *J. Aerosp. Eng.*, **11**(2), 52-58. https://doi.org/10.1061/(ASCE)0893-1321(1998)11:2(52)

Cheng, F.Y. and Jiang, H. (1998b), "Optimum control of a hybrid system for seismic excitations with state observer technique", *Smart Mater. Struct.*, **7**(5), 654. https://doi.org/10.1088/0964-1726/7/5/009

Cheng, F.Y., Jiang, H. and Lou, K. (2008), *Smart Structures: Innovative Systems for Seismic Response Control*, CRC Press, Boca Raton, FL, USA.

Chopra, A.K. (2017), *Dynamics of Structures. Theory and Applications to Earthquake Engineering*, Prentice-hall International Series, NY, USA.

Chung, L.L., Reinhorn, A.M. and Soong, T.T. (1988), "Experiments on active control of seismic structures", *J. Eng. Mech.*, **114**(2), 241-256. https://doi.org/10.1061/(ASCE)0733-9399(1988)114:2(241)

Chung, L.L., Lin, R.C., Soong, T.T. and Reinhorn, A.M. (1989), "Experimental study of active control for MDOF seismic structures", *J. Eng. Mech.*, **115**(8), 1609-1627. https://doi.org/10.1061/(ASCE)0733-9399(1989)115:8(1609)

Constantinou, M.C. and Symans, M.D. (1992), "Experimental and analytical investigation of seismic response of structures with supplemental fluid viscous dampers", National Center for Earthquake Engineering Research, Buffalo, NY, USA.

Constantinou, M.C., Tsopelas, P., Hammel, W. and Sigaher, A.N. (2001), "Toggle-brace-damper seismic energy dissipation systems", *J. Struct. Eng.*, **127**(2), 105-112. https://doi.org/10.1061/(ASCE)0733-9445(2001)127:2(105)

Council, B.S.S. (2000), "Prestandard and commentary for the seismic rehabilitation of buildings", Report FEMA-356, Washington, DC, USA.

De Domenico, D. and Ricciardi, G. (2018), "Earthquake protection of existing structures with limited seismic joint: base isolation with supplemental damping versus rotational inertia", *Adv. Civil Eng.*, **2018**. https://doi.org/10.1155/2018/6019495

Dinh, V.N., Basu, B. and Nagarajaiah, S. (2016), "Semi-active control of vibrations of spar type floating offshore wind turbines", *Smart Struct. Syst., Int. J.*, **18**(4), 683-705. https://doi.org/10.12989/sss.2016.18.4.683

Dyke, S.J., Spencer Jr, B.F., Belknap, A.E., Ferrell, K.J., Quast, P. and Sain, M.K. (1994a), "Absolute acceleration feedback control strategies for the active mass driver", *Proceedings of the 1st World Conference on Structural Control*, Pasadena, CA, USA.

Dyke, S.J., Spencer, B.F., Quast, P., Sain, M.K., Kaspari, D.C. and Soong, T.T. (1994b), *Experimental Verification of Acceleration Feedback Control Strategies for an Active Tendon System*, NCEER, USA.

Dyke, S.J., Spencer Jr, B.F., Quast, P., Kaspari Jr, D.C. and Sain, M.K. (1996a), "Implementation of an active mass driver using acceleration feedback control", *Comput.-Aid. Civil Infrastruct. Eng.*, **11**(5), 305-323. https://doi.org/10.1111/j.1467-8667.1996.tb00445.x

Dyke, S.J., Spencer Jr, B.F., Quast, P., Sain, M.K., Kaspari Jr, D.C. and Soong, T.T. (1996b), "Acceleration feedback control of MDOF structures", *J. Eng. Mech.*, **122**(9), 907-918. https://doi.org/10.1061/(ASCE)0733-9399(1996)122:9(907)

Fisco, N.R. and Adeli, H. (2011), "Smart structures: part I—active and semi-active control", *Scientia Iranica*, **18**(3), 275-284. https://doi.org/10.1016/j.scient.2011.05.034

Fu, F. (2018), *Design and Analysis of Tall and Complex Structures*, Butterworth-Heinemann, Oxford, UK.

Gharebaghi, S.A. and Zangooei, E. (2017), "Chaotic particle swarm optimization in optimal active control of shear buildings", *Struct. Eng. Mech., Int. J.*, **61**(3), 347-357. https://doi.org/10.12989/sem.2017.61.3.347

He, J., Xu, Y.L., Zhang, C.D. and Zhang, X.H. (2015), "Optimum control system for earthquake-excited building structures with minimal number of actuators and sensors", *Smart Struct. Syst., Int. J.*, **16**(6), 981-1002. https://doi.org/10.12989/sss.2015.16.6.981

Hejazi, F., Shoaei, M.D., Tousi, A. and Jaafar, M.S. (2016), "Analytical model for viscous wall dampers", *Comput.-Aid. Civil Infrastruct. Eng.*, **31**(5), 381-399. https://doi.org/10.1111/mice.12161

Housner, G., Bergman, L.A., Caughey, T.K., Chassiakos, A.G., Claus, R.O., Masri, S.F., Skelton, R.E., Soong, T.T., Spencer, B.F. and Yao, J.T. (1997), "Structural control: past, present, and future", *J. Eng. Mech.*, **123**(9), 897-971.

https://doi.org/10.1061/(ASCE)0733-9399(1997)123:9(897)

Hwang, J.S., Huang, Y.N., Hung, Y.H. and Huang, J.C. (2004), "Applicability of seismic protective systems to structures with vibration-sensitive equipment", *J. Struct. Eng.*, **130**(11), 1676-1684. https://doi.org/10.1061/(ASCE)0733-9445(2004)130:11(1676)

Hwang, J.S., Huang, Y.N. and Hung, Y.H. (2005), "Analytical and experimental study of toggle-brace-damper systems", *J. Struct. Eng.*, **131**(7), 1035-1043. https://doi.org/10.1061/(ASCE)0733-9445(2005)131:7(1035)

Ikeda, Y., Sasaki, K., Sakamoto, M. and Kobori, T. (2001), "Active mass driver system as the first application of active structural control", *Earthq. Eng. Struct. Dyn.*, **30**(11), 1575-1595. https://doi.org/10.1002/eqe.82

Jamnani, H.H., Abdollahzadeh, G. and Faghihmaleki, H. (2017), "Seismic fragility analysis of improved RC frames using different types of bracing", *J. Eng. Sci. Technol.*, **12**(4), 913-934.

Jamnani, H.H., Amiri, J.V. and Rajabnejad, H. (2018), "Energy distribution in RC shear wall-frame structures subject to repeated earthquakes", *Soil Dyn. Earthq. Eng.*, **107**, 116-128. https://doi.org/10.1016/j.soildyn.2018.01.010

Kareem, A., Kijewski, T. and Tamura, Y. (1999), "Mitigation of motions of tall buildings with specific examples of recent applications", *Wind Struct., Int. J.*, **2**(3), 201-251. https://doi.org/10.12989/was.1999.2.3.201

Liu, D.K., Yang, Y.L. and Li, Q.S. (2003), "Optimum positioning of actuators in tall buildings using genetic algorithm", *Comput. Struct.*, **81**(32), 2823-2827. https://doi.org/10.1016/j.compstruc.2003.07.002

Lu, Z., Li, J. and Jia, C. (2018), "Studies on energy dissipation mechanism of an innovative viscous damper filled with oil and silt", *Sustainability*, **10**(6), 1-13. https://doi.org/10.3390/su10061777

Mahdavi, N., Ahmadi, H.R. and Mahdavi, H. (2012), "A comparative study on conventional push-over analysis method and incremental dynamic analysis (IDA) approach", *Scientif. Res. Essays*, **7**(7), 751-773.

Majeed, A.P.A. Taha, Z. Abdullah, M.A., Azmi, K.Z.M. and Zakaria, M.A. (2018), "The control of an upper extremity exoskeleton for stroke rehabilitation: An active force control scheme approach", *Adv. Robot. Res., Int. J.*, **2**(3), 237-245. https://doi.org/10.12989/arr.2018.2.3.237

Miah, M.S., Chatzi, E.N. and Weber, F. (2015), "Semi-active control for vibration mitigation of structural systems incorporating uncertainties", *Smart Mater. Struct.*, **24**(5), 055016. https://doi.org/10.1088/0964-1726/24/5/055016

Muthalif, A.G., Kasemi, H.B., Nordin, N.H., Rashid, M.M. and Razali, M.K.M. (2017), "Semi-active vibration control using experimental model of magnetorheological damper with adaptive F-PID controller", *Smart Struct. Syst., Int. J.*, **20**(1), 85-97. https://doi.org/10.12989/sss.2017.20.1.085

Pakar, I., Bayat, M. and Cveticanin, L. (2018), "Nonlinear vibration of unsymmetrical laminated composite beam on elastic foundation", *Steel Compos. Struct., Int. J.*, **26**(4), 453-461. https://doi.org/10.12989/scs.2018.26.4.453

Pantelides, C.P. and Cheng, F.Y. (1990), "Optimal placement of controllers for seismic structures", *Eng. Struct.*, **12**(4), 254-262. https://doi.org/10.1016/0141-0296(90)90024-M

Park, W., Park, K.S., Koh, H.M. and Ha, D.H. (2006), "Wind-induced response control and serviceability improvement of an air traffic control tower", *Eng. Struct.*, **28**(7), 1060-1070. https://doi.org/10.1016/j.engstruct.2005.11.013

Park, W., Park, K.S. and Koh, H.M. (2008), "Active control of large structures using a bilinear pole-shifting transform with H∞ control method", *Eng. Struct.*, **30**(11), 3336-3344. https://doi.org/10.1016/j.engstruct.2008.05.009

Rao, A.R.M. and Sivasubramanian, K. (2008), "Optimal placement of actuators for active vibration control of seismic excited tall buildings using a multiple start guided neighbourhood search (MSGNS) algorithm", *J. Sound Vib.*, **311**(1-2), 133-159. https://doi.org/10.1016/j.jsv.2007.08.031

Ras, A. and Boumechra, N. (2016), "Seismic energy dissipation study of linear fluid viscous dampers in steel structure design", *Alexandria Eng. J.*, **55**(3), 2821-2832. https://doi.org/10.1016/j.aej.2016.07.012

Reinhorn, A.M., Viti, S. and Cimellaro, G. (2005), "Retrofit of structures: Strength reduction with damping enhancement", *Proceedings of the 37th UJNR Panel Meeting on Wind and Seismic Effects*.

Ricciardelli, F., Pizzimenti, A.D. and Mattei, M. (2003), "Passive and active mass damper control of the response of tall buildings to wind gustiness", *Eng. Struct.*, **25**(9), 1199-1209. https://doi.org/10.1016/S0141-0296(03)00068-3

Şigaher, A.N. and Constantinou, M.C. (2003), "Scissor-jack-damper energy dissipation system", *Earthq. Spectra*, **19**(1), 133-158. https://doi.org/10.1193/1.1540999

Soong, T.T. (1988), "State-of-the-art review: active structural control in civil engineering", *Eng. Struct.*, **10**(2), 74-84. https://doi.org/10.1016/0141-0296(88)90033-8

Soong, T.T. and Dargush, G.F. (1997), *Passive Energy Dissipation Systems in Structural Engineering*, John Wiley & Sons.

Soong, T.T. and Spencer Jr, B.F. (2002), "Supplemental energy dissipation: state-of-the-art and state-of-the-practice", *Eng. Struct.*, **24**(3), 243-259. https://doi.org/10.1016/S0141-0296(01)00092-X

Spencer Jr, B.F. and Nagarajaiah, S. (2003), "State of the art of structural control", *J. Struct. Eng.*, **129**(7), 845-856. https://doi.org/10.1061/(ASCE)0733-9445(2003)129:7(845)

Spencer, B.F. and Sain, M.K. (1997), "Controlling buildings: a new frontier in feedback", *IEEE Control Syst. Maz.*, **17**(6), 19-35. https://doi.org/10.1109/37.642972

Spencer, B.F., Dyke, S.J., Sain, M.K. and Quast, P. (1993), "Acceleration feedback control strategies for a seismic protection", *Proceedings of American Control Conference*, San Francisco, CA, USA, June. https://doi.org/10.23919/ACC.1993.4793085

Taylor, D.P. (1999a), U.S. Patent No. 5,870,863. Washington, DC: U.S. Patent and Trademark Office.

Taylor, D.P. (1999b), U.S. Patent No. 5,934,028. Washington, DC: U.S. Patent and Trademark Office.

Tian, Z., Mokrani, B., Alaluf, D., Jiang, J. and Preumont, A. (2017), "Active tendon control of suspension bridges: Study on the active cables configuration", *Smart Struct. Syst., Int. J.*, **19**(5), 463-472. https://doi.org/10.12989/sss.2017.19.5.463

Wu, B., Ou, J.P. and Soong, T.T. (1997), "Optimal placement of energy dissipation devices for three-dimensional structures", *Eng. Struct.*, **19**(2), 113-125. https://doi.org/10.1016/S0141-0296(96)00034-X

Xu, Y.L. and Teng, J. (2002), "Optimum design of active/passive control devices for tall buildings under earthquake excitation", *Struct. Des. Tall Build.*, **11**(2), 109-127. https://doi.org/10.1002/tal.193

Xu, H.B., Zhang, C.W., Li, H., Tan, P., Ou, J.P. and Zhou, F.L. (2014), "Active mass driver control system for suppressing wind-induced vibration of the Canton Tower", *Smart Struct. Syst., Int. J.*, **13**(2), 281-303. https://doi.org/10.12989/sss.2014.13.2.281

Yamamoto, M., Aizawa, S., Higashino, M. and Toyama, K. (2001), "Practical applications of active mass dampers with hydraulic actuator", *Earthq. Eng. Struct. Dyn.*, **30**(11), 1697-1717. https://doi.org/10.1002/eqe.88

Yamazaki, S., Nagata, N. and Abiru, H. (1992), "Tuned active dampers installed in the Minato Mirai (MM) 21 Landmark Tower in Yokohama", *J. Wind Eng. Ind. Aerodyn.*, **43**(1-3), 1937-1948. https://doi.org/10.1016/0167-6105(92)90618-K

Yang, J.N. and Soong, T.T. (1988), "Recent advances in active control of civil engineering structures", *Probabil. Eng. Mech.*, **3**(4), 179-188. https://doi.org/10.1016/0266-8920(88)90010-0

Zhan, M., Wang, S., Yang, T., Liu, Y. and Yu, B. (2017), "Optimum design and vibration control of a space structure with the hybrid semi-active control devices", *Smart Struct. Syst., Int. J.*, **19**(4), 341-350. https://doi.org/10.12989/sss.2017.19.4.341

CC